EJN European Journal of Neuroscience

FENS Federation of European Neuroscience Societies

European Journal of Neuroscience, Vol. 46, pp. 1906–1917, 2017 doi:10.1111/ejn.13568

CLINICAL AND TRANSLATIONAL NEUROSCIENCE

Motor deficits and beta oscillations are dissociable in an alpha-synuclein model of Parkinson's disease

Ivani Brys,[1,2] Jessica Nunes[3,4] and Romulo Fuentes[3,5]
[1]Psychobiology Post Graduation Program, Federal University of Rio Grande do Norte, Natal, Brazil
[2]Federal University of Vale do São Francisco, Petrolina, Brazil
[3]Edmond e Lily Safra Institute of Neuroscience, Natal, Brazil
[4]Physical Education Department, Potiguar University, Natal, Brazil
[5]Biomedical Sciences Institute, Universidad de Chile, Santiago, Chile

Keywords: beta oscillations, corticostriatal circuit, high-frequency oscillations, local field potential, spinal cord stimulation

Edited by Jochen Roeper
Received 27 January 2015, revised 27 February 2017, accepted 24 March 2017

Abstract

Parkinson's disease (PD) is a neurodegenerative disorder characterised by progressive motor symptoms resulting from chronic loss of dopaminergic neurons in the nigrostriatal pathway. The over expression of the protein alpha-synuclein in the substantia nigra has been used to induce progressive dopaminergic neuronal loss and to reproduce key histopathological and temporal features of PD in animal models. However, the neurophysiological aspects of the alpha-synuclein PD model have been poorly characterised. Hereby, we performed chronic *in vivo* electrophysiological recordings in the corticostriatal circuit of rats injected with viral vector to over express alpha-synuclein in the right substantia nigra. Our model, previously shown to exhibit mild motor deficits, presented moderate dopaminergic cell loss but did not present prominent local field potential oscillations in the beta frequency range (11–30 Hz), considered a hallmark of PD, during the 9 weeks after onset of alpha-synuclein over expression. Spinal cord stimulation, a potential PD symptomatic therapy, was applied regularly from sixth to ninth week after alpha-synuclein over expression onset and had an inhibitory effect on the firing rate of corticostriatal neurons in both control and alpha-synuclein hemispheres. Dopamine synthesis inhibition at the end of the experiment resulted in severe parkinsonian symptoms such as akinesia and increased beta and high-frequency (>90 Hz) oscillations. These results suggest that the alpha-synuclein PD model with moderate level of dopaminergic depletion does not reproduce the prominent corticostriatal beta oscillatory activity associated to parkinsonian conditions.

Introduction

Parkinson's disease (PD) is a neurodegenerative disorder associated to the progressive loss of dopaminergic neurons in the nigrostriatal pathway (Eriksen *et al.*, 2009) and the gradual emergence of different symptoms, including motor impairment. Available pharmacological and neuromodulation approaches provide symptomatic relief for PD motor deficits, but to date there is no available methods to cure, halt or even slow down the progression of PD.

Extensive preclinical research on PD has been done in the commonly used 6-hydroxydopamine (6-OHDA) model, in which the microinjection of this compound in the striatum or the medial forebrain bundle partially or totally destroys nearby dopaminergic projections and neurons, causing parkinsonian motor deficit. However, the 6-OHDA model does not reproduce key aspects of PD, such as formation of protein aggregates, progressive neural destruction, and gradual and sustained emergence of symptoms over long periods of time.

Recently, alpha-synuclein over expression by direct injection of viral vectors carrying the gene for human alpha-synuclein in the substantia nigra of rats has been used to model PD. Alpha-synuclein is the major component of the Lewy bodies (Recchia *et al.*, 2004), the cytoplasmic inclusions found in neurons of the nigrostriatal pathway and locus coeruleus that are considered a key cellular hallmark of PD (Schulz-Schaeffer, 2010). Nigral alpha-synuclein over expression leads to progressive neuronal degeneration of the nigrostriatal pathway (Kirik *et al.*, 2002; Decressac

Correspondence: R. Fuentes, Programa de Fisiología y Biofísica, ICBM, Facultad de Medicina, Universidad de Chile, Av. Independencia 1027, Santiago 8389100, Chile.
E-mail: romulo.a.fuentes@gmail.com

Address(es) from which the work originated: Edmond and Lily Safra Institute of Neuroscience of Natal Prof. Francisco Luciano de Oliveira, 2460 – Candelária 59066-060 – Natal, RN, Brazil; Psychology Faculty, Federal University of Vale do São Francisco, Av. José de Sá Maniçoba, s/n – Centro – Petrolina, Brazil 56304-917; Programa de Fisiología y Biofísica, ICBM, Facultad de Medicina, Universidad de Chile, Av. Independencia 1027, Santiago, Chile 8389100 –7

et al., 2012a), that is, preceded by axonal damage and impairments in the release and reuptake of dopamine in the presynaptic terminals (Lundblad *et al.*, 2012). Furthermore, the alpha-synuclein over expression causes other pathogenic features of PD, such as an inflammatory response (Chung *et al.*, 2009) and impairment of the synaptic function (Lundblad *et al.*, 2012). A comparative study between the 6-OHDA and the alpha-synuclein models concluded that the latter replicates PD more closely (Decressac *et al.*, 2012a). Motor symptoms of the alpha-synuclein model can be alleviated by standard pharmacological PD approach, and as recently demonstrated, by novel approaches such spinal cord stimulation (Brys *et al.*, 2016).

In addition to the histopathological hallmarks and symptomatology, PD can also be characterised by its neurophysiologic features. One of the most ubiquitous is the high degree of synchrony of neuron populations from motor circuits, which can be measured as increased oscillations of the local field potential (LFP) in specific frequency bands (Schnitzler & Gross, 2005). In PD patients, electrophysiological recordings of the subthalamic nucleus (STN) show increased synchronous oscillatory activity in the 13–35 Hz beta band (Kühn *et al.*, 2006; Weinberger *et al.*, 2009). The occurrence of increased neural synchrony in PD is associated to decreased dopamine levels. In animal models, major changes in the dopamine levels heavily impact the neuronal activity of the corticostriatal circuit. For example, hyperdopaminergic state in mice is associated with asynchronous neuronal activity and hyperkinesia, while severe dopamine depletion is related to akinesia and highly synchronous low frequency in the range 1.5–4 Hz (delta band) and 11–30 Hz (beta band) activity in the cortex and striatum (Costa *et al.*, 2006). 6-OHDA lesions of midbrain result in increased beta (22–32 Hz) oscillatory activity of frontal cortex and STN from rats (Sharott *et al.*, 2005). Recordings in globus pallidus and STN from MPTP-treated monkeys also revealed an increased oscillatory burst activity in frequencies around 10 Hz (Heimer *et al.*, 2006; Wichmann & Soares, 2006).

Pathological increased neural synchrony can be reduced by pharmacological and neuromodulation PD therapy approaches in human patients and animal models. Levodopa increases dopamine levels and reduces subthalamic low-frequency oscillations, which is accompanied by improvement in rigidity and bradykinetic symptoms (Kühn *et al.*, 2006). In a similar way, deep brain stimulation (DBS) also disrupts beta oscillations in the STN and cortical-STN beta coherence during motor improvement (Wingeier *et al.*, 2006; Kuhn *et al.*, 2008). Spinal cord stimulation (SCS), more recently proposed as a potential PD therapy, improves motor activity and reduces synchronous low-frequency activity in the cortico-basal-ganglia circuits of 6-OHDA rodent and marmoset models of PD (Fuentes *et al.*, 2009; Santana *et al.*, 2014). The correlation between the absence of synchronic neural activity and the alleviation of motor symptoms has led to the notion that the exaggerated low-frequency neural synchrony could be part of the mechanisms mediating the motor symptoms in parkinsonism (Eusebio *et al.*, 2012).

While the parkinsonian increased neural synchrony in beta frequency band is well described in the 6-OHDA and MPTP models, it is unknown if the alpha-synuclein model also reproduces these electrophysiological alterations. If exacerbated low-frequency neural beta oscillations are correlated with the progression of PD, it is expected that the alpha-synuclein model would exhibit the emergence of increasing amounts of beta oscillatory power over time. To test this prediction, we performed chronic *in vivo* electrophysiological recordings in the striatum and motor cortex in rats injected with AAV6 vector to over express the human protein alpha-synuclein in the substantia nigra. To further explore the neuroelectrophysiology of this model, we tested on it the effects of spinal cord stimulation and at the end of the experiment, we challenged the alpha-synuclein model with further dopamine synthesis inhibition followed by levodopa administration.

Materials and Methods

Animals

Six adult male Sprague-Dawley rats (Chemistry Department, São Paulo University) were individually housed with laboratory chow and water *ad libitum* in a 22–24 °C temperature room and a controlled 12 h light/dark cycle (lights on from 0700 h to 1900 h). National and institutional guidelines for animal welfare were followed and all procedures were approved by the Ethics Committee of the Associação Alberto Santos Dumont para Apoio à Pesquisa, Natal/Brazil, protocol #12/2011. As shown in Fig. 1A, experiments were performed with all animals at the same time to minimise possible effects of environmental and condition variables. By reducing potential external sources of variability, we aimed minimise the number of animals used in the study. Animals were weighed three times a week and at any signal of weight loss or pain, they received proper treatment from a technical veterinary.

Spinal cord stimulation electrodes

Custom-made stimulation electrodes consisted of 2 platinum bands: 3 × 0.9 mm (platinum foil thickness 25 μm, ©Goodfellow) positioned parallel to each other. Each band was connected with solder to a thin stainless steel wire (teflon-coated 7-strand, 0.012 inches, A-M Systems, Sequim, WA) at the upper surface. The assembled components were covered with surgical silicon, leaving the lower surface exposed. A surgical suture was secured between the platinum bands and used to tie the electrode to the vertebra to prevent electrode migration.

Recording electrode arrays

S-isonel-coated tungsten wire electrodes (50 μm) (California Fine Wire Co., CA) were configured into four arrays (16 × 4) with 250 μm spacing in each dimension and cut in two different lengths, corresponding the distances to the dorsolateral striatum (DLS) and the motor cortex (M1). The wires were connected to a circuit board attached to a connector (Omnetics Connector Corporation, Minneapolis, MN). Finally, the whole ensemble was fixed with UV-curing resin, Fig. 1B.

Viral vector preparation

AAV vectors pseudotyped with the serotype-6 capsid were prepared as previously described (Löw *et al.*, 2013). AAV2/6 particles were produced by transient transfection of the pDP6 and pAAV-pgk-β-globin intron-WPRE plasmids in 293-AAV cells. The empty pAAV-pgk-β-globin intron-WPRE construct was used to produce the non-coding control AAV2/6 particles, and the pAAV-pgk-β-globin-α-synuclein-WPRE plasmid was used to generate particles encoding human wild-type alpha-synuclein. AAV2/6 particles were isolated on an iodixanol step gradient followed by HPLC purification on heparin-binding columns. Finally, the vectors were concentrated and resuspended in phosphate buffer saline

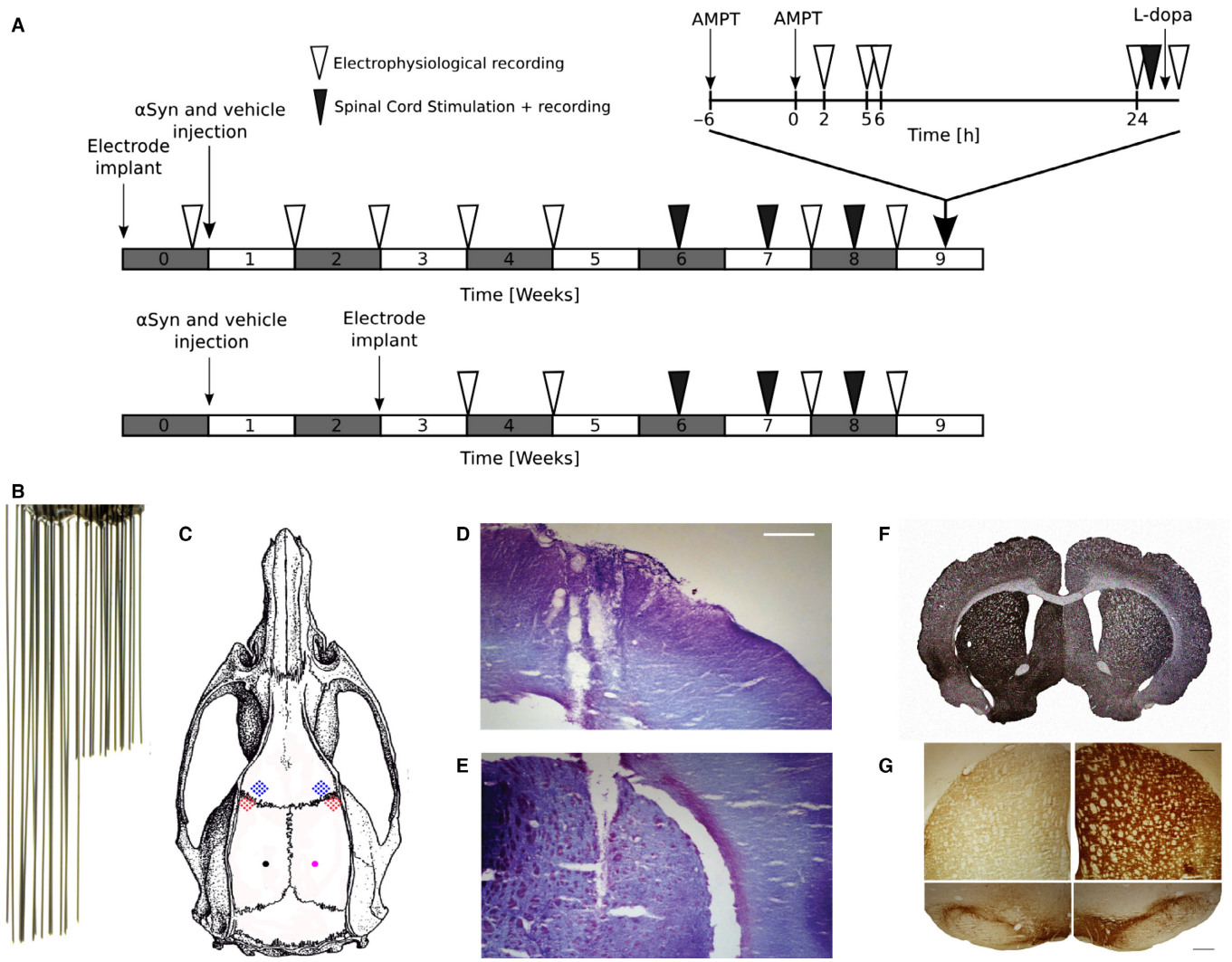

FIG. 1. Experimental design. (A) A group of rats (G1, $n = 3$) was bilaterally implanted with two multi-electrode recording arrays shown in (B) and a week later received an alpha-synuclein viral vector injection in the right substantia nigra and a vehicle injection in the left one. Electrophysiological recording sessions were conducted regularly according to the timing and conditions showed in the diagram. Another group of rats (G2, $n = 3$) received the electrode implant after the vehicle and alpha-synuclein vector injections thus were recorded starting week 3 after injection. At the end of week 9 (inset at upper right corner), all rats received a dose of AMPT (500 mg/kg), were recorded 2, 5, 6, and 24 h later. After the rats received a L-dopa injection (8 mg/kg), were recorded again and finally received spinal cord stimulation (SCS). (B) Thirty-two single microwire array for chronic electrophysiological extracellular recording in a single hemisphere. The shorter group of wires reached primary motor cortex (M1) and the longer reached dorsolateral striatum (DLS), and each group of wires was arranged in a squared shape. (C) Precise insertion locations of the two 32-wires arrays in the rat skull for M1 (blue dots) and DLS (red dots), also the location of the alpha-synuclein viral vector (magenta single dot) and sham injections (black single dot) to substantia nigra are shown. Nissl staining of brain slice showing the tracking of the electrodes in M1 (D) and DLS (E) (Scale bar: 500 μm). (F) Alpha-synuclein striatal expression 3 weeks after viral vector injection. (G) Right panel shows TH immunostaining after 9 weeks of alpha-synuclein expression in both control and expression hemisphere. Dopaminergic denervation can be observed in both striatum and substantia nigra, scale bars: 500 μm.

(PBS) to a volume of approximately 100 μL using Centricon Plus-20 filtration devices (100 000 MWCO, Millipore, Billerica, MA).

The relative infectivity titre of the vectors was measured by transducing HEK293T cells with serial dilutions of the vectors. The number of intracellular double-stranded vector genomes per cell, determined by real-time PCR, was used an indicator of the amount of transducing units (TU) as described in Dusonchet e al.

Vector injection

Under isoflurane (5% induction and 1% maintenance, Cristália, Sao Paulo, Brazil) anaesthesia, animals were injected with 2 μL (0.2 μL/min) of the empty vector suspension AAV6 in the left substantia nigra and the vector carrying the gene for wild-type human alpha-synuclein (6.09×10^{10} TU/mL, PBS, pH = 7.2) in the right substantia nigra: (AP): −5.2 mm; medio-lateral (ML): ±2.0 mm; and dorso-ventral (DV): −7.8 mm (relative to Bregma. 0 is set at the surface of the skull, Fig. 1C). A 32 G needle and a 5 μL glass Hamilton syringe were used for the injections. The needle was left *in situ* for five additional minutes and withdrawn slowly, to avoid backtracking of the suspension.

Spinal cord stimulation electrode and recording electrode implant

Animals were anaesthetised with ketamine (25 mg/kg, Syntec, Santana de Parnaiba, Brazil), xylazine (2.5 mg/kg, Syntec, Santana de

Parnaiba, Brazil), atropine (0.05 mL, Fagra, São Paulo, Brazil) and isoflurane (5% induction and 0.5% maintenance) and the SCS electrode was inserted in the epidural space under the second thoracic vertebra (T2) as previously described (Fuentes *et al.*, 2009). Both stimulation and recording electrodes were implanted in the same surgical procedure. Recording electrodes arrays were implanted in both hemispheres in the area corresponding to forelimbs at the following coordinates: M1: AP: 1.5 mm, ML: 2.8 mm; DV: −1.0 mm, Striatum: AP: 0.2 mm, ML: 3.8 mm; DV: −3.0 mm from cortical surface, Fig. 1D, E.

Electrophysiological recordings

The recordings (89 in total) were weekly performed in freely moving rats in an open field arena (86 × 66 cm; 39 sessions), during the pharmacological experiments (30 sessions) and the SCS sessions (20 sessions), as shown in Fig. 1A. Local field potentials (LFPs) and unitary activity (spikes) were acquired using a Multichannel Acquisition Processor (MAP) (Plexon Inc., US-TX). The signal to obtain the LFPs was amplified (300× or 3000×), filtered (0.7–170 Hz or 0.7–300 Hz) and digitised at 1000 Hz. To obtain the spike components the signal was amplified and band-pass filtered (154 Hz–8.8 kHz) and digitised at 40 kHz. Epochs of 0.8 ms duration (waveforms) around events greater than a threshold set by the operator were saved for offline sorting.

Spinal cord stimulation sessions

Animals underwent high-frequency spinal cord stimulation sessions (biphasic squared pulses, 400 μs duration each phase, delivered at 300 Hz for 30 min with a 4-channel general-purpose stimulus generator (STG4004 Multichannel Systems MCS GmbH, Reutlingen, Germany) once a week from 6th to 9th week after vector injection in the open field arena. Before each session, the stimulation current intensities were determined for each rat. Briefly, three 10-s stimulation epochs at the same intensity (starting with 50 μA) were delivered every 10 s. If no response was observed from the rat, the intensity was increased 25 μA and a new stimulation series started. The intensity, at which head and/or vibrissae movements were consistently observed as response to stimulation, was determined as the sensory or paresthesia threshold and was used for the SCS session. Average SCS current intensity was 110 ± 14.8 μA applied during 30 min (3 × [5 min SCS Off, 5 min SCS On]).

Pharmacological tests

AMPT and levodopa injections

Nine weeks after the vector injection, animals were injected with 500 mg/kg i.p. of α-Methyl-DL-tyrosine methyl ester hydrochloride (AMPT [initial dose 300 mg/kg followed by an injection of 200 mg/kg 6 h later, Sigma]). In the following day, rats were injected with levodopa 8 mg/kg (plus benserazide 15 mg/kg, Sigma).

Neuronal activity spike sorting and firing rate analysis

Neuronal activity (extracellular recorded spikes) was acquired during the recording sessions corresponding to 1st, 2nd, 3rd, 4th, 7th, 8th and 9th week, recording sessions 2, 5, 6 and 24 h after the first AMPT dose administration, during SCS, and after levodopa administration. To sort the spikes as belonging to individual neuronal units, the spike waveforms were clustered automatically with modified algorithms from the Chronux toolbox (Mitra & Bokil, 2008). The clusters were modified only by merging or splitting them according to the hierarchy imposed by the algorithm. Clusters with refractory periods and plausible waveforms were selected as potential units. Of these, units with spikes causing inter-spike intervals shorter than 1.6 ms were removed. The recording sessions previous to the vector injection had very few units, thus these were discarded from unit analysis. To classify the neuronal units as putative projection neurons or interneurons, the 32 points of the average waveform of each unit were used as input to a principal component analysis (PCA). The units were clustered according to the first and second components of the PCA using the unweighted average distance (UPGMA) method and represented as a scatter plot. For each area, two clusters were identified with distinct waveforms and firing rates. Units with wider spike waveforms and low firing rates were regarded as projection neurons, and units with shorter spike waveforms and higher firing rates were regarded as interneurons, likely fast spiking interneurons. We did not use a classification based on waveform duration parameters (peak-to-valley, peak width), since we lack the unfiltered waveforms (see Gage *et al.*, 2010 for comparison between filtered and unfiltered waveforms). After classification, units that showed session average firing rate above three standard deviations then described for that particular type, were discarded (see Gage *et al.*, 2010, for a table with the values).

For firing rate analysis during weekly recording sessions, the average firing rate of the complete session (30 min) was considered. For firing rate analysis during SCS, the average firing rate of each of the six 5-min periods of each recording session [off-on-off-on-off-on] was calculated by dividing the number of discharge time stamps by the exact duration of the period.

Local field potential analysis

Fixed-frequency artefacts of the LFP signals were removed after identifying them with independent components analysis (The FastICA package(C), 1996–2005 by Hugo Gävert, JarmoHurri, Jaakko Särelä, and Aapo Hyvärinen). Channels that still presented artefacts after this procedure were excluded from further analysis. Local bipolar LFP time series were computed offline from all unique pairs of electrodes from the same structure. Power spectral densities (PSDs) were calculated with seven tapers (Mitra & Bokil, 2008), a window length of 4 s, and a window overlap of 50%. PSDs were normalised to the pink noise background according to Halje *et al.* (2012). As a result, PSD values are represented as deviations from the pink noise floor in terms of the unit "pink dB".

Tissue preparation and immunohistochemistry

Nine weeks after the viral vector injection, animals were deeply anaesthetised with a dose of sodium pentobarbital (50 mg/kg) and transcardially perfused with 0.9% saline and ice cold 4% paraformaldehyde. Brains were removed and post fixed in paraformaldehyde 4% for 2 h. After that, brains were transferred to phosphate buffer (PB, pH = 7.4) 0.1 M for 12 h and 30% sucrose in PBS (pH = 7.2) at 4 °C for cryoprotection until they sank. The tissue was sectioned using a cryostat in 50 μm coronal slices and mounted on charged slides.

Cresyl violet staining

The position of the electrodes was confirmed by Cresyl violet staining, Fig. 1D, E. Sections were dehydrated with 99%, 85% and 70% EtOH (Sigma) for 3 min each, rinsed in dH2O for 5 min and then stained with 0.1% cresyl violet (CV, Sigma) powder in dH2O and

0.3% acetic acid (Sigma) solution for 5 min. Sections were then immersed in 50%, 70% and 99% EtOH for 1 min each, and 100% xylene (Sigma) for 5 min (2x).

Alpha-synuclein and Tyrosine Hydroxylase (TH) staining

Immunohistochemistry for alpha-synuclein was performed using a sheep polyclonal antibody generated using as antigen a synthetic peptide corresponding to amino acids 116–131 of the human alpha-synuclein that recognises both human and rat alpha-synuclein (dilution 1:1000, AB5334P Chemicon®, EMD Millipore). Briefly, sections were rinsed in 0.02 M PBS (2 × 10 min, pH = 7.2), 0.3% hydrogen peroxide diluted in PBS (20 min) to block endogenous peroxidase activity, and then washed 2 × 10 min in PBS. The sections were then incubated for 1 h at room temperature in a normal rabbit serum block solution containing 3% rabbit serum and 0.4% Triton X-100 diluted in PBS, followed by incubation with primary antibody for 48 h. Sections were rinsed in 0.02 M PBS (3 × 10 min) and incubated with biotinylated secondary antibody (1 : 500, Vector) for 2 h.

For TH immunohistochemistry, sections were unfrozen, washed in PB 0.1 M (5 min), hydrogen peroxide 0.3% diluted in methanol (20 min) and PBS/Tween 0.05% (5 min). Sections were then incubated in 10% normal goat TH serum (PBS) for 30 min, followed by incubation with primary antibody rabbit anti-TH (1 : 500, Chemicon) overnight. On the following day, sections were rinsed in PBS/Tween 0.05% (5 min) and incubated with biotinylated goat anti-rabbit antibody (1:200 in PBS, Vector) for 2 h.

After incubation with secondary antibody, all sections were rinsed in PBS/Triton 1% (alpha-synuclein) or PBS/Tween 0.05% (TH) for 5 min and incubated in avidin-biotin complex (ABC Kit, Vector). Subsequently, sections were rinsed in PBS/Tween 5% or PBS/Triton 1% (5 min) and stained with 3,3-diaminobenzidine and H2O2 (plus Nickel Chloride 1% for alpha-synuclein).

Cell counting

TH positive nigral neurons were quantified in both control and alpha-synuclein hemispheres in three sections from −5.7 to −4.8 AP (n = 6 rats) using a Nikon microscope with 40× magnification and the Stereo Investigator software.

Data analysis

The CinePlex® Behavioral Research System (Plexon Inc., US-TX) was used to perform video-tracking. Data were extracted using a custom-made algorithm for Matlab. Data were compared using repeated measures analysis of variance (RM ANOVA), Friedman and two tailed t-tests. Results are showed as Mean ± SEM. Statistical analyses were performed using the software Statistical Package for the Social Sciences (SPSS), version 21. The significance criterion was $P < 0.05$.

Results

Alpha-synuclein over expression resulted in moderate dopaminergic loss and did not affect corticostriatal population firing rate nor local field potential oscillatory power

The injection of the viral vector carrying the gene for wild-type human alpha-synuclein in the substantia nigra resulted in over expression of alpha-synuclein in the striatum (Fig. 1F), indicating the occurrence of anterograde transport of the alpha-synuclein in the nigrostriatal dopaminergic projections 3 weeks after the virus injection. Nine weeks after the viral vector injection, alpha-synuclein expression resulted in loss of tyrosine hydroxylase immunostaining, indicating loss of dopaminergic neurons (Fig. 1G). On average, alpha-synuclein over expression resulted in 48.5 ± 4.3% loss of nigral cells [$t(10) = 3.02$, $P < 0.05$, $n = 6$].

Chronic *in vivo* extracellular electrophysiological recording allowed us to collect single neuron activity and local field potentials 1 week before and for 9 weeks after the viral vector injection. Figure 2A shows an example of *in vivo* neuronal unit recording from one out of 64 implanted electrodes, were we were able to isolate six neurons (Fig. 2A). During the regular recording sessions across weeks, we recorded and isolated 370 neuronal units. On the basis of the average waveform of each unit, we classified them into putative groups in each recorded area: interneurons and projection neurons (see details in the Methods section). To this end, clustering was performed over the first and second principal components of the waveforms values, (Fig. 2B and C), resulting in 81 putative projection neurons from the dorsolateral striatum (DLS) (average ± SEM firing rate 5.3 ± 2.4 Hz), and 114 putative fast spiking DLS interneurons (FSI, firing rate 19.1 ± 15.1 Hz). In motor cortex – M1, we identified fix putative projection neurons (firing rate 4.1 ± 2.1 Hz) and 170 interneurons (firing rate 18.9 ± 16.2 Hz). The average firing rate values for each neuronal type are compatible with previously reported values (see Gage *et al.*, 2010 for comparison). To detect firing rate changes in the synuclein expressing areas, we represented the session average firing rates of all the neuronal units recorded in each hemisphere over up to 9 weeks after viral vector injection, but no consistent differences were observed following alpha-synuclein expression (Fig. 2D).

As stated earlier, increased oscillatory synchronic neural activity is a hallmark of PD, therefore, we looked for augmented beta power or any changes in other frequency bands (up to 70 Hz) in the local field potential (LFP) oscillations from motor cortex and dorsolateral striatum before and during the 9 weeks following the alpha-synuclein vector injection in the substantia nigra. The example in Fig. 3A shows the spectrograms from alpha-synuclein and control motor cortex and dorsolateral striatum from a single rat across time. While this example suggests, there are apparent changes over time (i.e. compare week 1 and 2), no overt differences are observed between injected and alpha-synuclein expressing areas (compare within each column, first to third and second to fourth row). Yet, this example reveals a clear difference in oscillatory power depending on the locomotive status of the rat. During the periods when the rat is not moving in an open field arena, there is an increase in oscillatory power around 10 Hz, which disappears when the rat is moving (Fig. 3B). Thus, to compare oscillatory power between alpha-synuclein and control sides, we considered only the periods of immobility. Group average LFP spectral power density did not show any significant differences in the oscillatory activity in the range 0.5–70 Hz between alpha-synuclein and control sides (Fig. 3C).

High-frequency spinal cord stimulation inhibits unitary activity in the corticostriatal circuit of synuclein model

We further investigated the electrophysiological effects of spinal cord stimulation (SCS), proposed as symptomatic treatment for PD, in the alpha-synuclein model. Animals received SCS once a week (from week 6–9) and *in vivo* electrophysiological recordings were performed during the stimulation sessions. No units were identified at week 9 and only data from weeks 6, 7 and 8 are displayed. First, we confirmed that SCS did not interfere with our ability to record

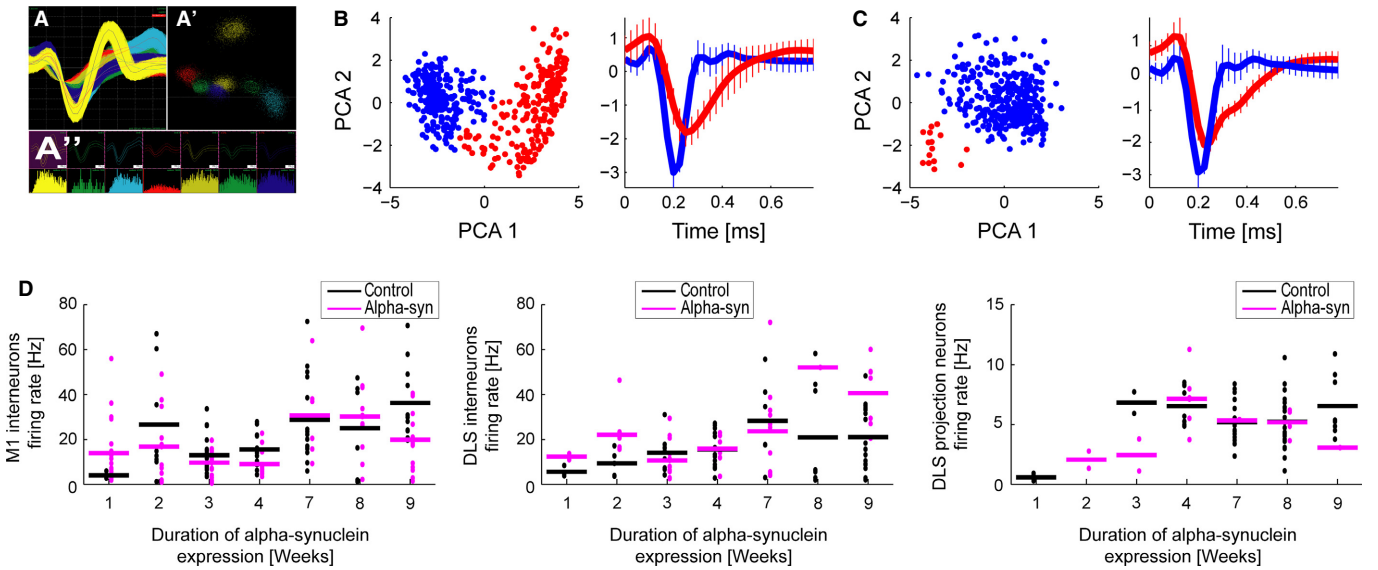

FIG. 2. Unitary corticostriatal activity. (A, A′, A″) Example of unitary neuronal sorting from a single channel as displayed in sorting software Offline Sorter ×64 V4 (Plexon Inc., Dallas) only for display purposes as actual sorting was done with custom algorithms (see Methods). (A) Simultaneously recorded waveforms in a single channel during a session, each colour representing a group of waveforms classified as belonging to the same unit. (A′) represents distinctive clusters formed by each unit when the first and second principal components of the waveforms are plotted against each other. (A″) Average waveform for each unit (top row) with the respective inter-spike interval distribution (bottom row). (B) Classification of all the DLS sorted neurons into putative interneurons and projection neurons based on clustering over the first and second components (left) of the average waveform of each unit, and (right) population average ± standard deviation of each population (red: projection neurons; blue: interneurons). (C) Classification of M1 sorted neurons in putative interneurons (blue) and projection neurons (red). (D) Average firing rate of neuronal units from control side (black dots) and alpha-synuclein side (magenta dots) over the weeks after viral vector expression. Horizontal lines represent the grand average. M1 projections neurons are not shown because of their low number.

and isolate unitary neuronal activity. In fact, stimulation artefacts from SCS at 300 Hz at different intensities were clear distinguishable and separable from the actual spikes (Fig. 4A). SCS at 300 Hz had a neuromodulatory effect in the activity of both M1 and DLS, with a clear predominance of inhibitory responses (Fig. 4B and C). No changes in relative power of LFP oscillations were observed during SCS delivery (data not shown).

Severe dopamine depletion by alpha-methyl-p-tyrosine injection results in increased beta activity in the corticostriatal circuit

To induce severe parkinsonian state, animals were subjected to pharmacological inhibition of tyrosine hydroxylase synthesis with alpha-methyl-p-tyrosine (AMPT) at 9th week after alpha-synuclein vector injection. This intervention caused decreased locomotive activity, and the emergence of strong LFP oscillatory activity in beta and high-frequencies (>90 Hz) ranges, exemplified in Fig. 5A. Overall, AMPT administration reduced the locomotive activity, measured as travelled distance, in all animals except one [$\chi^2(4) = 86.9$ $P = 0.1$, Friedman test, within subjects' variable: distance travelled in the open field]. At 2, 5, and 6 h after AMPT injection, there was an increase in the beta range (11–30 Hz) LFP oscillatory power spectral density only in the M1 expressing alpha-synuclein (Fig. 5B). This beta power increase was significant when compared to the control hemisphere and lasted for 24 h [$F_{1,10} = 6.1$, $P < 0.05$, RM ANOVA, within subjects factor: time; between subjects factor: side]. No significant changes in LFP oscillations between control and alpha-synuclein hemispheres were observed in DLS after AMPT injection (Fig. 5B, C). Twenty-four hours after AMPT injection, beta power decreased in M1 and DLS in both alpha-synuclein and control sides, yet in M1, beta power remained higher in the alpha-synuclein hemisphere. Levodopa administration and SCS are described to diminish the beta oscillations of parkinsonian conditions, thus, both treatments were tested in the alpha-synuclein + AMPT model. Neither the delivery of SCS nor levodopa administration diminished the 11–30 Hz LFP beta oscillations (Fig. 5B, C).

AMPT administration is associated with cortical high-frequency oscillations (HFO)

Beside the increase in beta oscillatory activity, AMPT administration resulted in the increase in LFP oscillations in two high-frequency bands. Five hours after AMPT injection, oscillatory activity with a peak at 120 Hz appeared in M1 and DLS in both control and alpha-synuclein sides (Fig. 5A, B). When this oscillation was evaluated across 115–145 Hz frequency range, it was significantly stronger in the M1 control side compared to M1 alpha-synuclein [$F_{1,10} = 20.3$, $P < 0.05$, RM ANOVA, within subjects factor: time; between subjects factor: side] (Fig. 5C). As the activity in the 115–145 Hz frequency range decreased over time after AMPT injection, another high-frequency band in the range 78–108 Hz with a peak at ~90 Hz became evident 24 h after AMPT administration [$F_{6,48} = 7.4$, $P < 0.05$, RM ANOVA, within subjects factor: time; between subjects factor: side] and was significantly stronger in the M1 control compared to M1 alpha-synuclein side [$F_{1,10} = 14.9$, $P < 0.05$, RM ANOVA, within subjects factor: time; between subjects factor: side], even after SCS delivery and levodopa administration Fig. 5A–C).

Discussion

Our data showed that moderate dopaminergic damage induced by alpha-synuclein over expression did not change neural population firing rate nor local field potential oscillatory activity in primary motor cortex and dorsolateral striatum. Increased LFP beta oscillations, considered a neurophysiological hallmark of PD, were

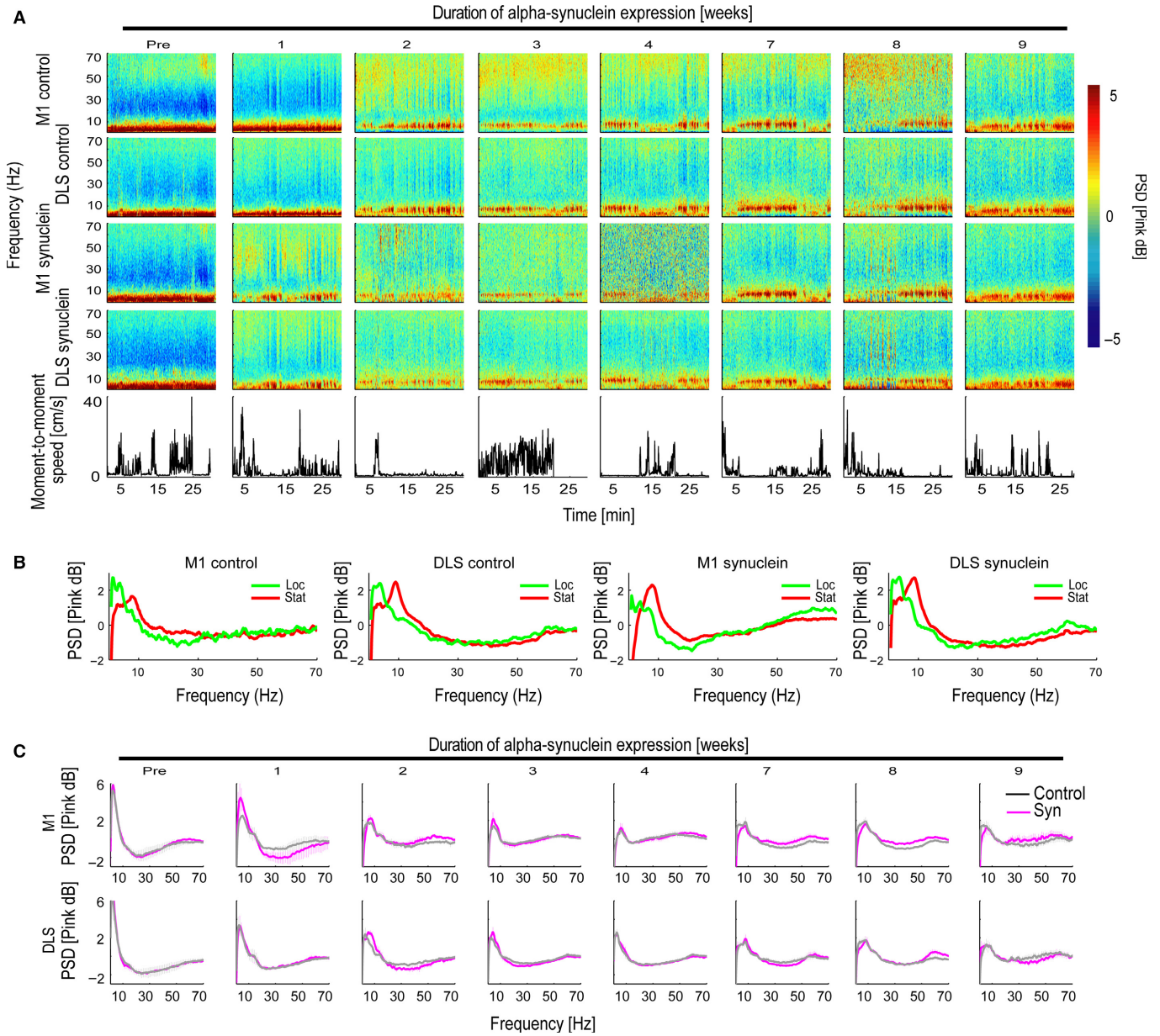

FIG. 3. Local Field potentials. (A) Example of spectrograms in M1 and DLS from recordings sessions 1 week before and 9 weeks after the viral vector injection to express alpha-synuclein. Each column corresponds to the spectrograms of control and injected M1 and DLS of a single recording session conducted ata specific week after the alpha-synuclein vector injection. Power spectral density is expressed in "pink dB" (see Methods). The moment-to-moment speed of the rat during the session is represented at the bottom of the figure. During periods of immobility (speed ~ 0 m/s), there is a power peak around 10 Hz (see weeks 3, 4, and 7), which disappears or decreases during the periods the rat is moving (speed > 0 cm/s).(B) Average power spectral density during locomotion ('Loc', green line) and immobility ('Stat', red line) periods in week 4. The latter presents increased power in beta range with a peak ~10 Hz. (C) Comparison of the average power spectral density during immobility periods between injected (magenta) and control (grey) M1 and DLS across weeks, vertical lines represent ±SEM (Pre-Week 2, $n = 3$; week 3–9, $n = 6$).

observed only after further dopamine depletion by AMPT administration. Unexpectedly, after AMPT administration two distinct high-frequency oscillations appeared which behaved differently in control and alpha-synuclein hemispheres. Early (5–6 h) after AMPT administration, high-frequency oscillations at 115–145 Hz appeared in M1, and were stronger in the control compared to the alpha-synuclein side. Twenty-four hours after AMPT administration, this oscillation faded, and another high-frequency oscillation appeared at 78–108 Hz, which was also stronger in the M1 control and weaker in the alpha-synuclein side.

Unilateral over expression of alpha-synuclein causes nigrostriatal degeneration and motor impairment, assessed as decreased use of the forelimb contralateral to the injection in the cylinder test (Decressac *et al.*, 2012b). Using the current protocol for alpha-synuclein over expression, in an earlier study, we observed a significant drop in the contralateral forepaw use, from around 50% before the injection, to around 20% 4 weeks after injection, and down to 10% 7 weeks after injection (Brys *et al.*, 2016). The recording cables hampered the vertical movements of the rats and we could not perform the cylinder test in the animals used in this study. However,

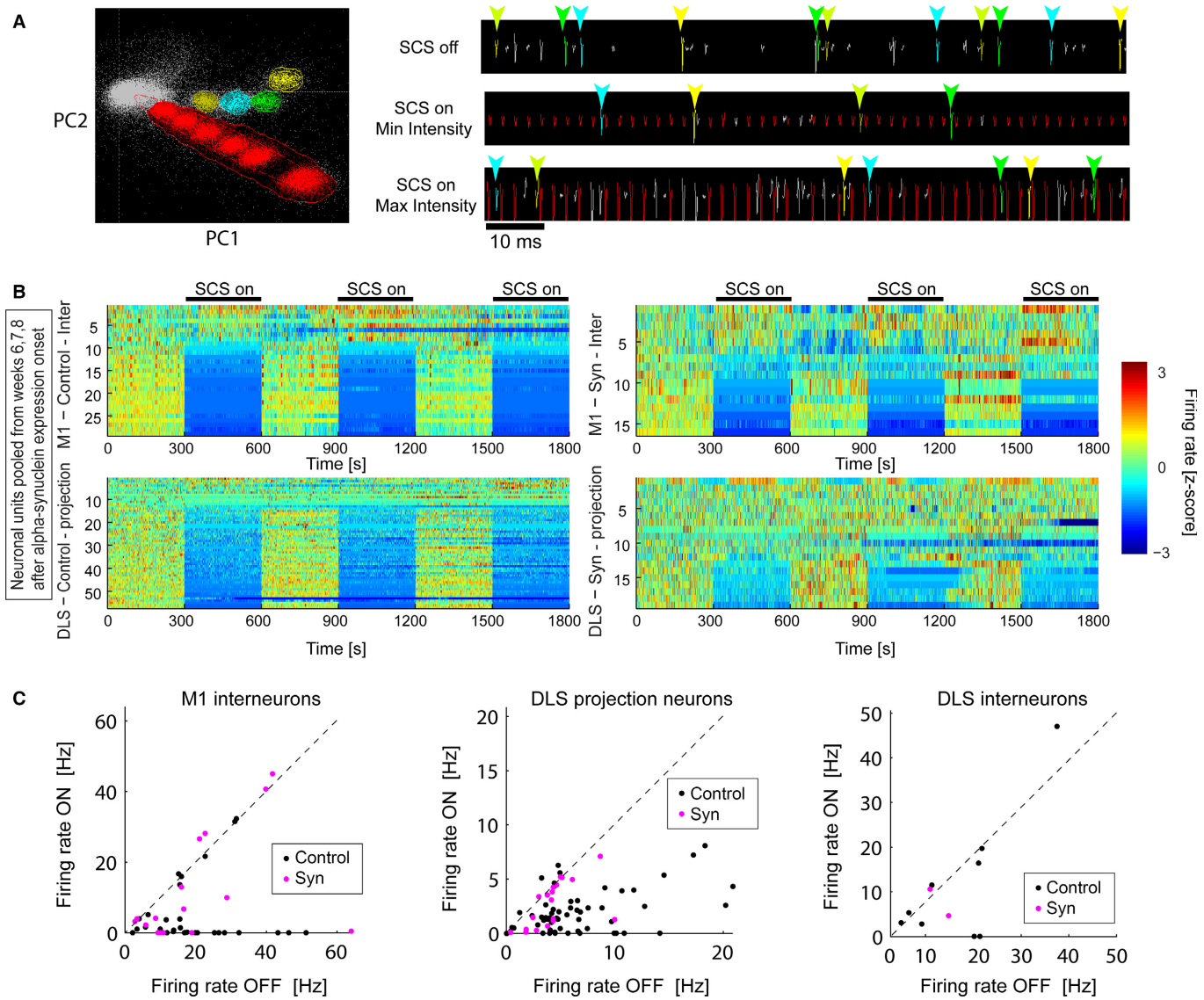

FIG. 4. High-frequency SCS inhibits neuronal firing in M1 and DLS. (A) Reliable neuronal unit recording and sorting can be achieved during spinal cord stimulation. Left: Standard algorithms used for spike clustering can easily separate action potentials from stimulation artefacts. The brown, cyano, green, and yellow clusters correspond to four neuronal units recorded while SCS was delivered in periods of increasing intensity. The red clusters correspond to the stimulation artefacts, grey dots correspond to unsorted spikes. Right: Examples of short recording periods (0.166 s) showing the action potentials of the four units during off stimulation (top), stimulation with minimum intensity (middle) and stimulation with maximum intensity (bottom). The action potentials of each neuron are labelled with an arrow head with the corresponding colour. The stimulation artefacts are not labelled and correspond to the red forms observed regularly in the middle and bottom panels. Grey forms correspond to unsorted data. The images were created with the software Offline Sorter ×64 V4 (Plexon Inc., Dallas) only for display purposes as actual sorting was done with custom algorithms. (B) The firing rate of 132 units recorded during weeks 6, 7 and 8 after vector injection (n = 5 rats) standardised to the first OFF period of the recording, is represented as a colour array (warm colours: increase over the mean OFF firing rate, cold colours: decrease relative to mean). SCS at 300 Hz was delivered during three epochs of 5-min each. Each row represents one neuron, and the total neurons were sorted according to descending standardised firing rate response to SCS. The black rectangles indicate the stimulation periods (SCS ON). (C) Firing rate in OFF epochs vs. ON epochs. Each dot represents the average firing rate response of a single unit across the three OFF and three ON epochs of all the sessions in control (black) and alpha-synuclein hemispheres (magenta). Regardless of the alpha-synuclein expression, two types of firing rate responses to SCS are observed: a minority of units with no changes (dots close to the dashed line) and a majority of units showing a decrease in firing rate during stimulation (dots under the dashed line).

given that exactly the same virus injection protocol was used and caused a similar percentage of cell loss in our previous study (43.5 ± 4.6% [Brys *et al.*, 2016], vs. 48.5 ± 4.3% in this study), it is expected that the animals of the current study had a similar level of motor impairment.

Although the unilateral alpha-synuclein model of this study presented moderate dopaminergic damage and likely motor impairment in the use of the contralateral forepaw, no firing rate changes or increased beta oscillations in the alpha-synuclein hemisphere were observed. Since this model assumes that the control condition for the unitary and LFP recordings is the hemisphere contralateral to the nigral alpha-synuclein expression, inter-hemisphere influence (i.e. the control side compensating the activity in the injected one, or an altering effect in the opposite direction) cannot be ruled out completely. Further investigation, with an experimental design that allows comparing between control and experimental subjects with

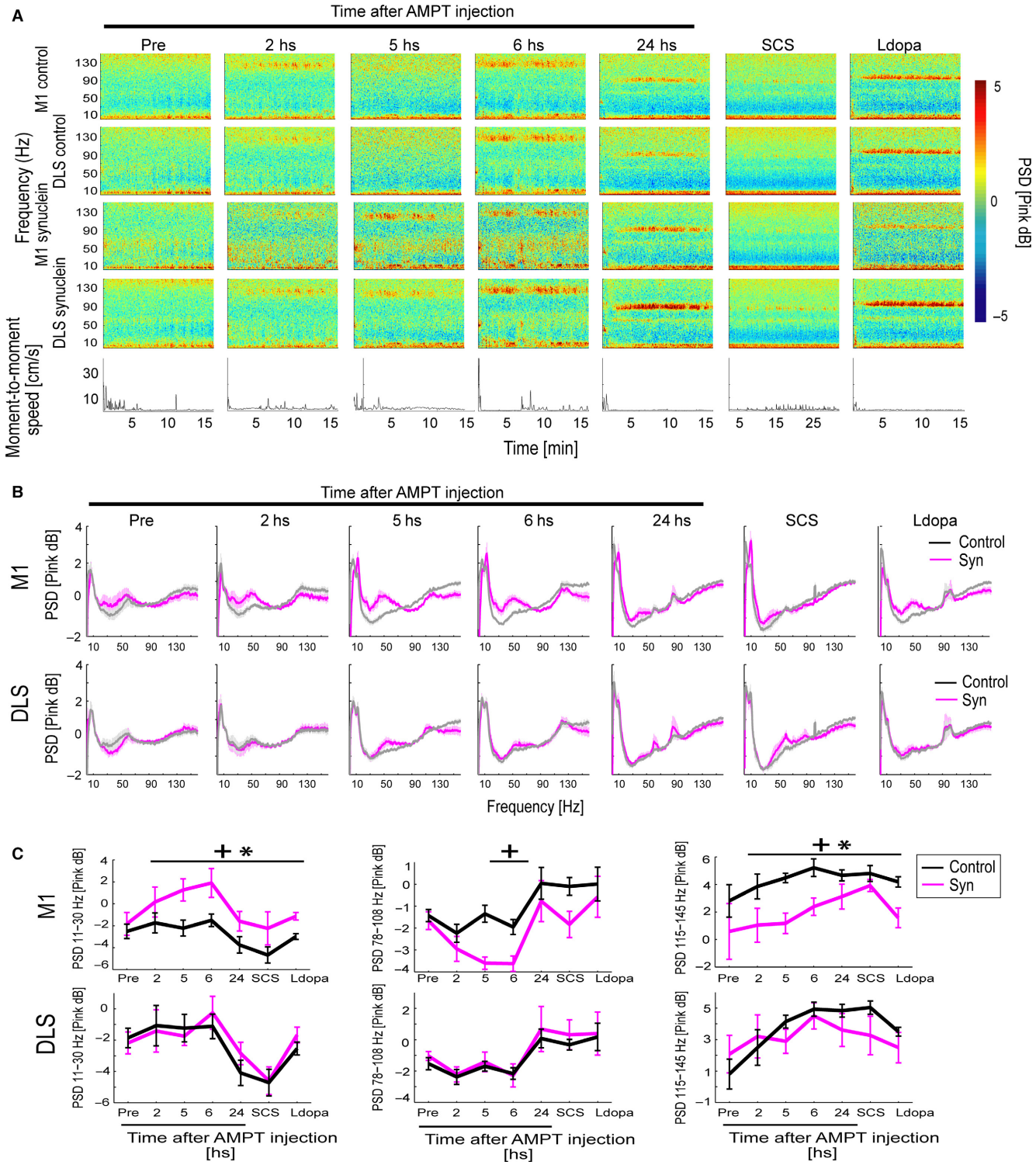

FIG. 5. Dopamine synthesis inhibitor AMPT results in severe parkinsonian condition in the alpha-synuclein PD model. (A) Example of changes in power spectral density in control and alpha-synuclein expressing M1 and DLS after the injection of the dopamine synthesis inhibitor AMPT. Each column corresponds to the spectrograms of a single recording session conducted in the indicated time after AMPT injection, the delivery of spinal cord stimulation (SCS) or levodopa injection. The moment-to-moment speed of the rat during the session is represented at the bottom. (B) Standardised power spectral density in M1 and DLS following 2, 5, 6 and 24 h after the administration of the tyroxine hydroxylase inhibitor AMPT, during SCS, and after levodopa administration (synuclein [magenta] and control [black trace], average ± SEM, n = 6 rats, except for 24 h after AMPT + SCS, where n = 5, because the stimulation wires were broken in one rat). The spectral power values were standardised against a recording done previously to the administration of AMPT. SCS was applied at low-intensity, during 3 × 5-min periods completing 15 min ON and 15 min OFF-stimulation. The spectral power values were standardised against a recording done previously to the administration of AMPT (regular recording session corresponding to week 9). The narrow peak at ~101 Hz in the 24 h after AMPT + SCS panel is a stimulation artefact present in four of the five stimulated rats (C) Changes in the power spectral density in the 11–30 Hz, 78–108 Hz and 115–145 Hz frequency bands. *Represents a significant difference between sides and + represents a significant difference over time, $P < 0.05$, RM ANOVA, within subjects factor: time; between subjects factor: side.

bilateral intervention is needed to further clarify this point. Such report in a transgenic alpha-synuclein model already exists and it supports our results (Lobb *et al.*, 2013). Lobb *et al.* reported that bilateral over expression of human alpha-synuclein in genetically modified mice caused motor deficit but no significant nigrostriatal dopamine denervation and, remarkably, it slightly decreased cortical beta activity [15–30 Hz]. This absence of increased beta oscillations in alpha-synuclein PD model adds to the set of evidence that correlates beta oscillations only with severe dopaminergic depletion and advanced PD patients, but not with moderate hypodopaminergic conditions (reviewed in Quiroga-Varela *et al.*, 2013). For example, complete 6-OHDA medial forebrain bundle (MFB) lesion causes 97% loss of TH immunostaining and augmented beta oscillations in the substantia nigra pars reticulata (SNpr) while a partial lesion or a progressive lesion (72 and 65% loss, respectively) do not, suggesting that severe dopaminergic denervation is necessary to produce neuronal hypersynchrony in the beta band (Quiroga-Varela *et al.*, 2013). Remarkably, recent experiments in the 6-OHDA model have been able to dissociate the increased beta oscillations from the motor symptoms: (i) pharmacological manipulations that suppress excessive subthalamic nucleus (STN) bursts (another PD neurophysiological hallmark) do alleviate bradykinesia, but do not decrease augmented STN and cortical beta oscillations; and (ii) a manipulation that increases STN burst occurrence causes bradykinesia but does not augment STN or cortical beta oscillations (Pan *et al.*, 2016).

In our study, electrical stimulation of the dorsal portion of the spinal cord was applied once a week starting at sixth week after alpha-synuclein vector injection. SCS has been shown to have therapeutic effects on motor symptoms in Parkinson's patients (Agari & Date, 2012; Fenelon *et al.*, 2012; Hassan *et al.*, 2013; Landi *et al.*, 2013; Arii *et al.*, 2014; Nishioka & Nakajima, 2015; Pinto de Souza *et al.*, 2016; but also see Thevathasan *et al.*, 2010). In animal models based on pharmacological dopamine depletion or 6-OHDA, SCS causes an acute improvement over motor deficit that is associated with a decrease in beta oscillatory activity across corticostriatal-thalamic motor circuits (Fuentes *et al.*, 2009; Santana *et al.*, 2014). We recently demonstrated that spinal cord stimulation has long-term therapeutic effects in an alpha-synuclein PD model alleviating motor asymmetry in the cylinder test (Brys *et al.*, 2016). In the current work SCS was applied following the same protocol of the previous study at very low intensities, starting the sixth week after the alpha-synuclein vector injection. While introducing a therapeutic intervention such as SCS in the last weeks of our experiment could prevent the appearance of significant electrophysiological changes, early in this model (3–4 weeks after onset of alpha-synuclein expression), when motor symptoms are already present (see Brys *et al.*, 2016), there are no electrophysiological changes in the alpha-synuclein hemisphere. This result is compatible with the evidence discussed earlier that suggests that increased beta neural synchrony appears only in severe, but not in moderate hypodopaminergic state (Quiroga-Varela *et al.*, 2013). Another evidence supporting this concept, is that mice over expressing and accumulating human alpha-synuclein under the control of Thy-1 promoter show motor deficits as early as 2-month age (Fleming *et al.*, 2004) but not increased, but rather slightly decreased, beta oscillations at 3–6 months age (Lobb *et al.*, 2013). During the delivery of SCS we did not observed changes in the LFP oscillatory activity, which was expected since our alpha-synuclein model in basal conditions (i.e. SCS OFF) did not present LFP oscillatory activity changes. Yet, SCS consistently caused an inhibitory effect on the unitary activity of neurons. This result is similar to the inhibitory effect observed with high-frequency deep brain stimulation (Vitek, 2002) and high-frequency SCS (Santana *et al.*, 2014). Although high-frequency stimulation of the subthalamic nucleus alleviates excessive cortical aberrant oscillations in 6-OHDA lesioned rats (Yang *et al.*, 2015), beta oscillations and the decreased locomotion did not respond to SCS in our extremely severe parkinsonian condition induced by AMPT, and nor did levodopa. This result suggests that a more specific or combined intervention is needed to restore motor functionality in a extreme severe parkinsonian condition, and it is congruent with previous studies where virtually 100% dopamine depleted DATKO mice do not respond to SCS until a minimum of levodopa is provided (Fuentes *et al.*, 2009).

Finally, tyrosine hydroxylase synthesis inhibition resulted in cortical high-frequency oscillations (HFO) occurring at two distinct peaks (~120 and ~90 Hz) in both lesioned and control hemispheres. In the 6-OHDA model, ~80 Hz cortical HFO have been associated with dyskinesia (Halje *et al.*, 2012; Tamtè *et al.*, 2016), a well described side effect of levodopa therapy (Winkler *et al.*, 2002). However, the HFOs described in the current work were not associated to exaggerated or involuntary movements but rather to complete immobility as observed in the open field arena. This, and the fact they are present at different frequency peaks than those reported by Halje *et al.* (2012), suggest that these HFO might be representing different phenomena.

Our experiments suggest that the progressive moderate dopaminergic impairment caused by alpha-synuclein expression did not cause any apparent electrophysiological change in the cortico striatal circuit at early states. In our study, differences between control and alpha-synuclein sides related to electrophysiological parkinsonian features, such as increased beta oscillations, were evident only when the circuit was challenged with further dopamine depletion. These evident electrophysiological changes were paralleled by overt motor impairment evidenced by significant decrease in locomotor activity in the open field arena.

Overall, the main result of this study, which is that no increased beta oscillations were found in the early stage of this alpha-synuclein model, suggests that augmented beta oscillations do not occur in moderate dopaminergic deficit, and it adds to the accumulating evidence that hints towards that augmented beta oscillations, while correlated with hypodopaminergic states, might not be part of the causal mechanisms of the motor impairment in PD.

Conflict of interests

Authors declare no competing interests.

Acknowledgements

IB received a doctorate fellowship from Coordenação de Aperfeiçoamento de Pessoal de Nível Superior (Capes). JN received a scientific initiation fellow ship from Conselho Nacional de Desenvolvimento Científico e Tecnológico (CNPq). The project was funded by the Swiss Brazilian Scientific & Technology Cooperation Fund (CNPq), the Instituto Nacional de Interface Cérebro-Máquina (704134/2009). RF was funded by NuMIND Millenium Nucleus No. NC130011, Fondecyt No. 1151478, and BNI Millennium Institute No. P09-015-F while analysing data and writing this manuscript. The authors would like to thank Bernard L. Schneider and Wojciech Bobela from Mind Institute, Ecole Polytechnique Fédérale de Lausanne for providing the viral vectors, Denis Matrov for the alpha-synuclein immunostaining, and the Brain Institute of UFRN for the use of microscopes to generate the alpha-synuclein immunostaining image.

Author contributions

IB and RF designed the experiments, wrote the manuscript and performed analysis. IB and JN performed the experiments.

Data accessibility

Data are not publicly available since they belong to the private non-profit institution Alberto Santos Dumont Association for Research Support (AASDAP) and are under a confidentiality agreement.

Abbreviations

6-OHDA, 6-hydroxydopamine; AAV, adenovirus; AP, anteroposterior; DBS, deep brain stimulation; DLS, dorsolateral striatum; DV, dorso-ventral; GLM-RM, repeated measures ANOVA; LFP, Local field potential; M1, motor cortex; ML, medio-lateral; PB, phosphate buffer; PBS, phosphate buffer saline; PD, Parkinson's disease; STN, subthalamic nucleus; TH, Tyrosine Hydroxylase; TU, transducing units.

References

Agari, T. & Date, I. (2012) Spinal cord stimulation for the treatment of abnormal posture and gait disorder in patients with Parkinson's Disease. *Neurol. Med. Chir.*, **52**, 470–474.

Arii, Y., Sawada, Y., Kawamura, K., Miyake, S., Taichi, Y., Izumi, Y., Kuroda, Y., Inui, T. *et al.* (2014) Immediate effect of spinal magnetic stimulation on camptocormia in Parkinson's disease. *J. Neurol. Neurosurg. Psychiatry*, **85**, 1221–1226.

Brys, I., Bobela, W., Schneider, B.L., Aebischer, P. & Fuentes, R. (2016) Spinal cord stimulation improves forelimb use in an alpha-synuclein animal model of Parkinson's disease. *Int. J. Neurosci.*, **7454**, 1–9.

Chung, C.Y., Koprich, J.B., Siddiqi, H. & Isacson, O. (2009) Dynamic changes in presynaptic and axonal transport proteins combined with striatal neuroinflammation precede dopaminergic neuronal loss in a rat model of AAV α-synucleinopathy. *J. Neurosci.*, **29**, 3365–3373.

Costa, R.M., Lin, S., Sotnikova, T.D., Cyr, M., Gainetdinov, R.R., Caron, M.G. & Nicolelis, M.A.L. (2006) Rapid alterations in corticostriatal ensemble coordination during acute dopamine-dependent motor dysfunction. *Neuron*, **52**, 359–369.

Decressac, M., Mattsson, B. & Björklund, A. (2012a) Comparison of the behavioural and histological characteristics of the 6-OHDA and α-synuclein rat models of Parkinson's disease. *Exp. Neurol.*, **235**, 306–315.

Decressac, M., Mattsson, B., Lundblad, M., Weikop, P. & Björklund, A. (2012b) Progressive neurodegenerative and behavioural changes induced by AAV-mediated overexpression of α-synuclein in midbrain dopamine neurons. *Neurobiol. Dis.*, **45**, 939–953.

Eriksen, N., Stark, A.K., Pakkenberg, B. (2009). Age and Parkinson's Disease-Related Neuronal Death in the Substantia Nigra Pars Compacta. In Di Giovanni, G., Di Matteo, V. & Esposito, E. (Eds), *Birth, Life and Death of Dopaminergic Neurons in the Substantia Nigra*. Springer, Vienna, pp. 203–213.

Eusebio, A., Cagnan, H. & Brown, P. (2012) Does suppression of oscillatory synchronisation mediate some of the therapeutic effects of DBS in patients with Parkinson's disease? *Front. Integr. Neurosci.*, **6**, 47.

Fenelon, G., Goujon, C., Gurruchaga, J.M., Cesaro, P., Jarraya, B., Palfi, S. & Lefaucheur, J.P. (2012) Spinal cord stimulation for chronic pain improved motor function in a patient with Parkinson's disease. *Parkinsonism Relat. D.*, **18**, 213–214.

Fleming, S.M., Salcedo, J., Fernagut, P.-O., Rockenstein, E., Masliah, E., Levine, M.S. & Chesselet, M.-F. (2004) Early and progressive sensorimotor anomalies in mice overexpressing wild-type human alpha-synuclein. *J. Neurosci.*, **24**, 9434–9440.

Fuentes, R., Petersson, P., Siesser, W.B., Caron, M.G. & Nicolelis, M.A.L. (2009) Spinal cord stimulation restores locomotion in animal models of Parkinson's disease. *Science*, **323**, 1578–1582.

Gage, G.J., Stoetzner, C.R., Wiltschko, A.B. & Berke, J.D. (2010) Selective activation of striatal fast-spiking interneurons during choice execution. *Neuron*, **67**, 466–479.

Halje, P., Tamte, M., Richter, U., Mohammed, M., Cenci, M.A. & Petersson, P. (2012) Levodopa-induced Dyskinesia is strongly associated with resonant cortical oscillations. *J. Neurosci.*, **32**, 16541–16551.

Hassan, S., Amer, S., Alwaki, A. & Elborno, A. (2013) A patient with Parkinson's disease benefits from spinal cord stimulation. *J. Clin. Neurosci.*, **20**, 1155–1156.

Heimer, G., Rivlin-Etzion, M., Bar-Gad, I., Goldberg, J.A., Haber, S.N. & Bergman, H. (2006) Dopamine replacement therapy does not restore the full spectrum of normal pallidal activity in the 1-methyl-4-phenyl-1,2,3,6-tetra-hydropyridine primate model of Parkinsonism. *J. Neurosci.*, **26**, 8101–8114.

Kirik, D., Rosenblad, C., Burger, C., Lundberg, C., Johansen, T.E., Muzyczka, N., Mandel, R.J. & Björklund, A. (2002) Parkinson-like neurodegeneration induced by targeted overexpression of alpha-synuclein in the nigrostriatal system. *J. Neurosci.*, **22**, 2780–2791.

Kuhn, A.A., Kempf, F., Brucke, C., Gaynor Doyle, L., Martinez-Torres, I., Pogosyan, A., Trottenberg, T., Kupsch, A. *et al.* (2008) High-frequency stimulation of the subthalamic nucleus suppresses oscillatory activity in patients with Parkinson's disease in parallel with improvement in motor performance. *J. Neurosci.*, **28**, 6165–6173.

Kühn, A.A., Kupsch, A., Schneider, G.-H. & Brown, P. (2006) Reduction in subthalamic 8-35 Hz oscillatory activity correlates with clinical improvement in Parkinson's disease. *Eur. J. Neurosci.*, **23**, 1956–1960.

Landi, A., Trezza, A., Pirillo, D., Vimercati, A., Antonini, A. & Sganzerla, E.P. (2013) Spinal cord stimulation for the treatment of sensory symptoms in advanced Parkinson's disease. *Neuromodulation*, **16**, 276–279.

Lobb, C.J., Zaheer, A.K., Smith, Y. & Jaeger, D. (2013) In vivo electrophysiology of nigral and thalamic neurons in alpha-synuclein-overexpressing mice highlights differences from toxin-based models of Parkinsonism. *J. Neurophysiol.*, **110**, 2792–2805.

Löw, K., Aebischer, P. & Schneider, B.L. (2013) Direct and retrograde transduction of nigral neurons with AAV6, 8, and 9 and intraneuronal persistence of viral particles. *Hum. Gene Ther.*, **24**, 613–629.

Lundblad, M., Decressac, M., Mattsson, B. & Björklund, A. (2012) Impaired neurotransmission caused by overexpression of α-synuclein in nigral dopamine neurons. *Proc. Natl. Acad. Sci.*, **109**, 3213–3219.

Mitra, P. & Bokil, H. (2008). *Observed Brain Dynamics*, 1st edn.. Oxford University Press, Oxford, USA.

Nishioka, K. & Nakajima, M. (2015) Beneficial therapeutic effects of spinal cord stimulation in advanced cases of Parkinson's disease with intractable chronic pain: a case series. *Neuromodulation*, **18**, 751–753.

Pan, M., Kuo, S., Tai, C., Liou, J., Pei, J., Chang, C., Wang, Y., Liu, W. *et al.* (2016) Neuronal firing patterns outweigh circuitry oscillations in parkinsonian motor control. *J. Clin. Invest.*, 1–11.

Pinto de Souza, C., Hamani, C., Oliveira Souza, C., Lopez Contreras, W.O., dos Santos Ghilardi, M.G., Cury, R.G., Reis Barbosa, E., Jacobsen Teixeira, M. *et al.* (2016) Spinal cord stimulation improves gait in patients with Parkinson's disease previously treated with deep brain stimulation. *Movement Disord*, **32**, 278–282.

Quiroga-Varela, A., Walters, J.R., Brazhnik, E., Marin, C. & Obeso, J.A. (2013) What basal ganglia changes underlie the parkinsonian state? The significance of neuronal oscillatory activity. *Neurobiol. Dis.*, **58**, 242–248.

Recchia, A., Debetto, P., Negro, A., Guidolin, D., Skaper, S.D. & Giusti, P. (2004) α-Synuclein and Parkinson's disease. *FASEB J.*, **18**, 617–626.

Santana, M., Halje, P., Simplício, H., Richter, U., Freire, M., Petersson, P., Fuentes, R. & Nicolelis, M.A.L. (2014) Spinal cord stimulation alleviates motor symptoms in a primate model of Parkinson's disease. *Neuron*, **84**, 716–722.

Schnitzler, A. & Gross, J. (2005) Normal and pathological oscillatory communication in the brain. *Nat. Rev. Neurosci.*, **6**, 285–296.

Schulz-Schaeffer, W.J. (2010) The synaptic pathology of α-synuclein aggregation in dementia with Lewy bodies, Parkinson's disease and Parkinson's disease dementia. *Acta Neuropathol.*, **120**, 131–143.

Sharott, A., Magill, P.J., Harnack, D., Kupsch, A., Meissner, W. & Brown, P. (2005) Dopamine depletion increases the power and coherence of beta-oscillations in the cerebral cortex and subthalamic nucleus of the awake rat. *Eur. J. Neurosci.*, **21**, 1413–1422.

Tamtè, M., Brys, I., Richter, U., Ivica, N., Halje, P. & Petersson, P. (2016) Systems-level neurophysiological state characteristics for drug evaluation in an animal model of levodopa-induced dyskinesia. *J. Neurophysiol.*, **115**, 1713–1729.

Thevathasan, W., Mazzone, P., Jha, A., Djamshidian, A., Dileone, M., Di Lazzaro, V. & Brown, P. (2010) Spinal cord stimulation failed to relieve akinesia or restore locomotion in Parkinson disease. *Neurology*, **74**, 1325–1327.

Vitek, J.L. (2002) Mechanisms of deep brain stimulation: excitation or inhibition. *Movement Disord*, **17**, S69–S72.

Weinberger, M., Hutchison, W.D. & Dostrovsky, J.O. (2009) Pathological subthalamic nucleus oscillations in PD: can they be the cause of bradykinesia and akinesia? *Exp. Neurol.*, **219**, 58–61.

Wichmann, T. & Soares, J. (2006) Neuronal firing before and after burst discharges in the monkey basal ganglia is predictably patterned in the normal state and altered in parkinsonism. *J. Neurophysiol.*, **95**, 2120–2133.

Wingeier, B., Tcheng, T., Koop, M.M., Hill, B.C., Heit, G. & Bronte-Stewart, H.M. (2006) Intra-operative STN DBS attenuates the prominent beta rhythm in the STN in Parkinson's disease. *Exp. Neurol.*, **197**, 244–251.

Winkler, C., Kirik, D., Björklund, A. & Cenci, M.A. (2002) l-DOPA-induced Dyskinesia in the intrastriatal 6-hydroxydopamine model of Parkinson's Disease: relation to motor and cellular parameters of nigrostriatal function. *Neurobiol. Dis.*, **10**, 165–186.

Yang, C., Zhang, J.-R., Chen, L., Ge, S.-N., Wang, J.-L., Yan, Z.-Q., Jia, D., Zhu, J.-L. *et al.* (2015) High frequency stimulation of the STN restored the abnormal high-voltage spindles in the cortex and the globus pallidus of 6-OHDA lesioned rats. *Neurosci. Lett.*, **595**, 122–127.